We are IntechOpen,
the world's leading publisher of
Open Access books
Built by scientists, for scientists

6,900
Open access books available

186,000
International authors and editors

200M
Downloads

154
Countries delivered to

Our authors are among the

TOP 1%
most cited scientists

12.2%
Contributors from top 500 universities

CLARIVATE ANALYTICS
BOOK CITATION INDEX
INDEXED

WEB OF SCIENCE™

Selection of our books indexed in the Book Citation Index
in Web of Science™ Core Collection (BKCI)

Interested in publishing with us?
Contact book.department@intechopen.com

Numbers displayed above are based on latest data collected.
For more information visit www.intechopen.com

Stereolithography

Christina Schmidleithner and Deepak M. Kalaskar

Additional information is available at the end of the chapter

Abstract

The stereolithography (SLA) process and its methods are introduced in this chapter. After establishing SLA as pertaining to the high-resolution but also high-cost spectrum of the 3D printing technologies, different classifications of SLA processes are presented. Laser-based SLA and digital light processing (DLP), as well as their specialized techniques such as two-photon polymerization (TPP) or continuous liquid interface production (CLIP) are discussed and analyzed for their advantages and shortcomings. Prerequisites of SLA resins and the most common resin compositions are discussed. Furthermore, printable materials and their applications are briefly reviewed, and insight into commercially available SLA systems is given. Finally, an outlook highlighting challenges within the SLA process and propositions to resolve these are offered.

Keywords: stereolithography (SLA), digital light processing (DLP), additive manufacturing (AM), 3D printing, two-photon polymerization (TPP), continuous liquid interface production (CLIP)

1. Introduction

As the oldest additive manufacturing (AM) technology, stereolithography (SLA) was first developed by Dr. Hideo Kodama in 1981. He saw it as a fast and low-cost method of reconstructing models in 3D space as an alternative to holographic techniques [1]. The first commercially available SLA printer was patented in 1986 by Charles W. Hull, who founded 3D Systems Inc. Their aim was to facilitate rapid prototyping of plastic parts [2]. With the development of a variety of processes, SLA has far surpassed its initial applications in modeling and prototyping and can be utilized to manufacture highly complex and individually designed geometries. The material is also no longer limited to conventional polymers, but the fabrication

	Resolution (μm)	Surface roughness (μm)	Sources
SLA	10–150	0.38–0.61	[6–8]
Material jetting	25–100	0.47–8.44	[6, 9]
Material extrusion	100–400	3.24–42.97	[6, 9]
Powder bed fusion	50–100	17–105	[7, 10]
Soft lithography	<0.01	<0.001	[9, 11]

Table 1. Comparison of average lateral resolution and surface roughness of AM technologies for polymers and of soft lithography.

of composites [3] and even metallic [4] or ceramic [5] specimens is possible. However, to date, SLA is only being utilized to structure one material at a time, and when comparing to other additive manufacturing (AM) technologies, typical SLA processes exhibit superior resolution and better surface qualities (see **Table 1**) but at slower printing times and higher cost.

While soft lithography is not an AM technology, it merits mentioning as a competing method due to its superior resolution to most SLA systems. It utilizes elastomeric stamps or molds to fabricate 3D structures and consequently does not have the characteristic advantages of 3D printing such as the ability of direct and rapid fabrication from a computer-aided design (CAD) model [12]. Nevertheless, it is often employed as an alternative to SLA in for example microfluidic applications [6].

2. The stereolithography setup

SLA is a vat polymerization method [13], where layers of the liquid precursor in a vat are sequentially exposed to ultraviolet (UV) light and thereby selectively solidified. A photo-initiator (PI) molecule in the resin responds to incoming light and upon irradiation, locally activates the chemical polymerization reaction, which leads to curing only in the exposed areas. After developing the first layer in that manner, a fresh resin film is applied, irradiated, and cured. Thus, the part incrementally grows layer-after-layer [1]. This principle spans all SLA processes, which can be classified according to the direction of incident light or irradiation method, see **Figure 1**.

The required light for solidification of the resin can be applied in two distinct manners; either from above in the free surface approach, or from below through a transparent vat in the constrained surface approach. Irradiation can either be implemented by scanning of each point of the desired cross-section with a laser in laser-SLA or by projecting the entire pixelated image onto the layer in digital light processing (DLP) SLA. A more uncommon method is illumination through an liquid crystal display (LCD) photomask.

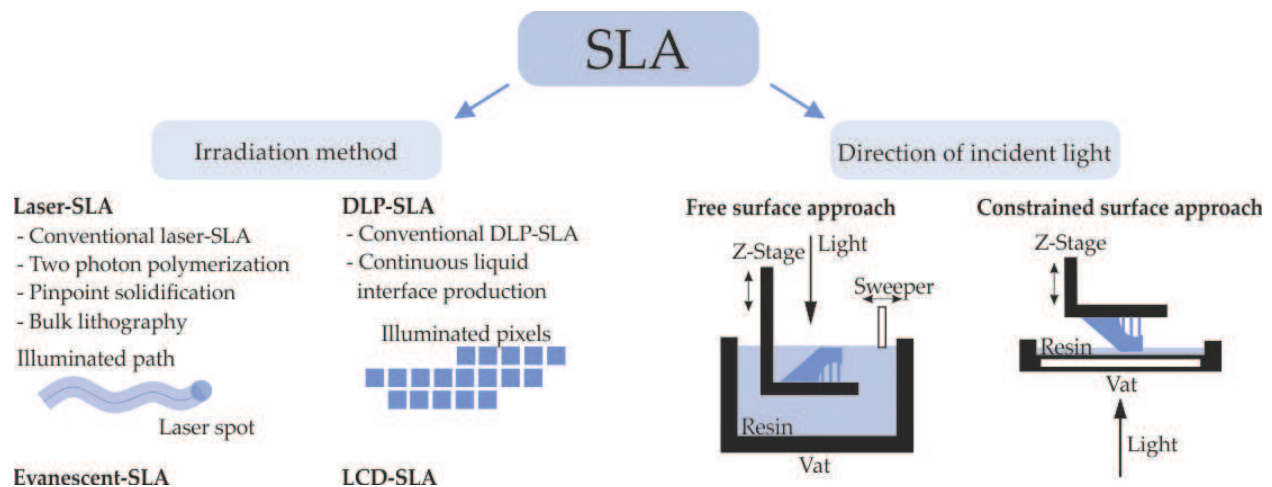These systems and some of their adaptations will be explained in detail in the following sections.

Figure 1. Classification of SLA according to irradiation method (left) and direction of incident light (right).

2.1. Free and constrained surface approach

In the **free surface approach**, the building platform on which the printed part grows is situated in a tank of resin and coated with a liquid resin film. Illumination of the desired cross-section, which happens from above the resin bath, cures the first layer. After each layer, the platform with the growing part (i.e. the z-stage), is lowered further into the tank, and new resin is coated on top with a mechanical sweeper. This sets the stage for the subsequent layer [14].

The **constrained surface approach** or bottom-exposure approach has a building platform, which can be suspended above the resin bath. Illumination from below, through the transparent floor, cures a layer of resin between building platform and vat floor. This layer adheres to the platform, as the z-stage is raised by a defined distance. As each layer is cured, the building platform with the adhered part is elevated, and the part grows suspended from the platform downward [6]. As with the free surface setup, support structures made from the same printing material are needed in case of overhangs and undercuts to ensure adequate adhesion to the platform.

Recently, there has been a trend toward the bottom-exposure approach, as it has certain advantages [6, 15, 16]. The smooth surface, which is created with a narrowly defined layer height due to the precise movement of the z-stage at an accuracy of down to 0.1–1 μm [17, 18], is the main benefit in the constrained surface setup. Without the need for a mechanical sweeper, this layer can be created faster than in the free surface approach, reducing the printing time [15]. Another advantage, which decreases cost, is the lower amount of resin that is needed because the specimen does not have to be completely submerged in the vat [14].

A main disadvantage of the bottom-exposure setup, however, is that attractive forces between printed part and vat floor need to be overcome for each layer [19]. When pulling up the z-stage, the newly cured layer needs to adhere to the layers above, and may not stick to the vat surface. Attempts to reduce this unwanted interaction include the application of hydrophobic coatings of the material tray [15, 18–20] and modification of the mechanical separation mechanism with tilting steps [21] or application of shear forces [20].

2.2. Laser-stereolithography

In Laser-SLA, also known as vector-based SLA, or often simply referred to as SLA, each layer is cured by scanning of a UV laser onto the resin film. This x-y motion of the laser is implemented by two galvanometers in combination with a dedicated optical system. An example of setup is given schematically in **Figure 2**. These conventional SLA devices, although more expensive than other AM technologies such as their extrusion-based counterparts, can reach resolutions of 5–10 μm [8].
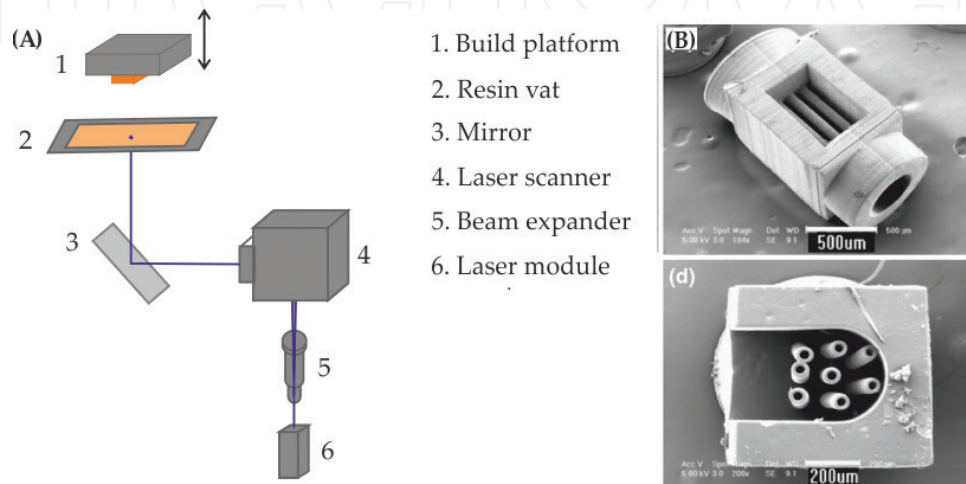

Figure 2. Schematic setup of a laser-SLA printer (A), adapted, and modified from [22]. Scanning electron microscope (SEM) images of a bioreactor with capillaries fabricated with laser-SLA (B), reprinted from [23] by permission of springer nature.

In order to attain these resolutions, a number of parameters need to be considered. Besides accuracy of the z-stage and optimized resin composition (see Section 3.3), which are important factors especially in z-resolution, the manner in which the UV laser is scanned across the desired layer is decisive. The geometry of the precisely defined laser lines, which illuminate the entire cross-section [24] and their accuracy, given by movement of the galvano-mirror, determine lateral resolution. Furthermore, the scanning speed and diameter of the laser spot need to be considered. They, respectively, influence the cure depth and width of the exposed laser lines and thereby affect vertical and lateral resolution [25]. Methods to further improve the resolution to sub-micron regions include two-photon polymerization (TPP) and pinpoint solidification.

2.2.1. Two-photon polymerization (TPP)

TPP was first proposed as an AM method by Strickler *et al.* [26]. As resolutions superior to 100 nm with surface roughness below 10 nm are attainable [27], it has been extensively studied since then [28], and despite its high-cost, TPP was even commercialized by Nanoscribe GmbH in 2007 [29].

In TPP, excitation of the PI in the resin, and thereby activation of the curing reaction, does not occur in the entire illumination path of the laser, as in conventional SLA, but only in the

region of its focal point, called a volume pixel or voxel [30]. A high-intensity femtosecond pulsed laser can cause molecules to absorb two photons simultaneously. As the probability of this phenomenon is proportional to the squared intensity of the laser pulse, the process is limited to the focal point of the laser. Instead of UV light, a laser at twice the wavelength (i.e. half the energy) with near-infrared (NIR) light such as a Titanium-sapphire laser is employed in TPP. The energy necessary for excitation is nevertheless attained by the combination of the energies of both individual photons [31].

As portrayed in **Figure 3**, the spatially constrained 3D voxel in TPP allows for curing of shapes inside the resin bath and not just on its surface. This eliminates the need for layer-wise production and enables fabrication of extremely complex geometries including freely moving parts without superfluous support structures [28].
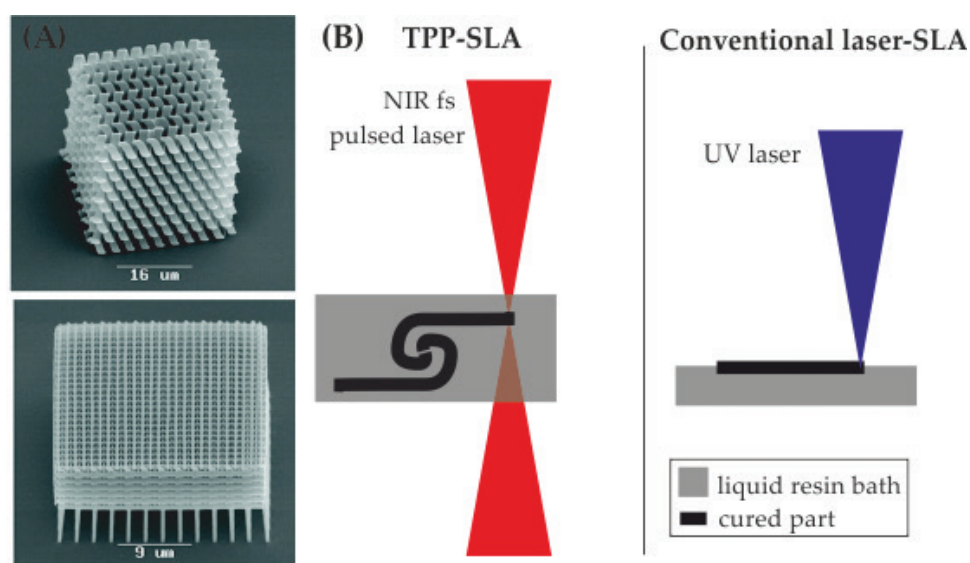

Figure 3. SEM images of microstructures fabricated with TPP (A), reprinted with permission from [32] (Ovsianikov A. et al. ultra-low shrinkage hybrid photosensitive material for two-photon polymerization microfabrication.), copyright (2008) American Chemical Society. Scheme of TPP vs. conventional laser-SLA (B) redrawn and adapted from [33].

One of the challenges which remain in TPP is the restriction to extremely small geometries in the mm range [34] and low writing speed of the laser lines. At a maximum of a few mm/s, it cannot compare to hundreds of mm/s, which is attainable with conventional laser-SLA methods [8]. Developing a suitable PI could help speed up the process. Conventional UV initiators have the drawback of low-activity in TPP. In order to augment their response, the design of molecules with specific structures is necessary [35].

2.2.2. Pinpoint solidification

A method similar to TPP, pinpoint solidification, was proposed by Ikuta *et al.* in 1998 under the name of super integrated hardened polymer SLA (Super IH) process [36]. A tightly focused laser is used and as with TPP, due to the high intensity in the focal point of the laser, curing of the resin can only be achieved in this voxel. The mechanism, however, is that of conventional single photon polymerization. Thus, resolutions of below 0.4 µm have been reached without

the use of expensive fs pulsed lasers [37]. This process has as of yet not been commercialized, and very little research is invested in pinpoint solidification-SLA.

2.2.3. Bulk lithography

In bulk lithography, 3D textures can be created by variation of exposure energy. The cure depth, which is a direct function of laser power or scan velocity (i.e. of the applied energy), thereby defines the depth of the features [38]. One can thus see the entire part as only existing of one layer with varying thickness. This eliminates the sometimes abrupt steps in z-direction, which are generated with conventional SLA methods, and vastly speeds up printing. Although this process is not capable of printing structures with overhangs and is limited to geometries thinner than 0.25 mm, it could have potential future applications in high-throughput fabrication of microstructures [39].

2.3. Digital light processing stereolithography

DLP is a method, which can reach resolutions in the order of 25 μm [7]. Smallest feature sizes of 0.6 μm have also been reported [40], and resins filled with ceramic particles have been printed via DLP with layer heights of 15 μm and with lateral resolutions of 40 μm [18].

In contrast to laser-SLA, the entire cross-section of a layer is illuminated simultaneously by a DLP light engine, as shown in **Figure 4**. The digital micromirror device (DMD) is the key component and functions as a dynamic mask for the DLP process. It is constructed of an array of mirrors, each one representing a single pixel. Individual tilting of every mirror enables fast and reliable switching of pixels [42]. When linked with a computer for image processing, a light source (often LED), and optics, it can project desired cross-sections of light quickly and precisely [42]. The fast switching speed of the DMD is a prerequisite for realizing grayscale illumination, which can be beneficial for precise control over exposure time and by extent energy dosage [40].
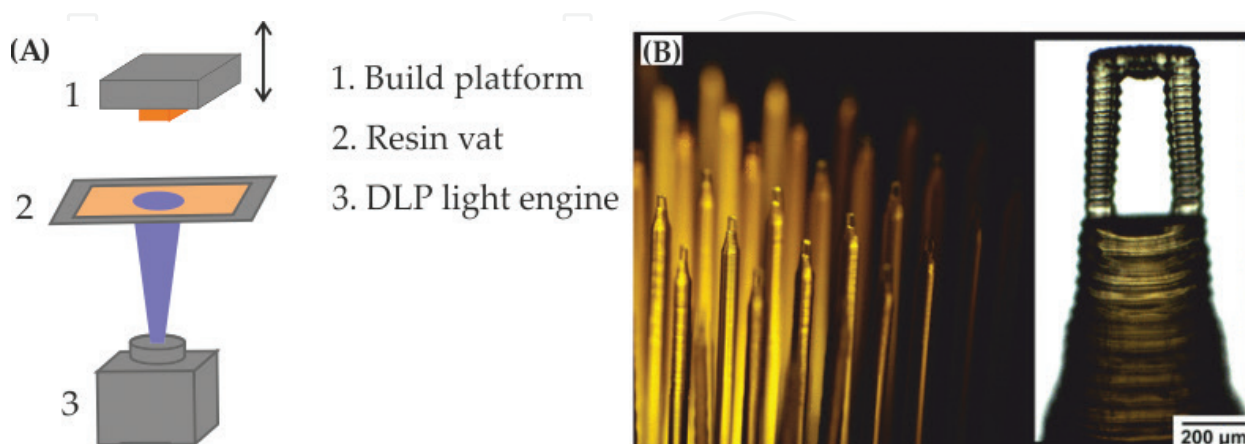

Figure 4. Setup of a DLP-SLA printer (A) adapted and redrawn from [22]. Printed polymer structures (B) adapted and reprinted with permission from [41] (Macdonald NP. et al., 3D printed micrometer-scale polymer mounts for single crystal analysis). Copyright (2017) American Chemical Society.

With its pixel-based exposure mechanism, DLP is excellent for illumination of sharp corners but can cause saw-tooth type surface roughness on otherwise curved surfaces [18]. Consequently, when aiming for higher resolution, the pixel size needs to be reduced with the help of designated optics. As the DMD has a fixed amount of mirrors, this leads to shrinkage of the image and reduces maximum geometry size. Large parts are thus often printed at lower resolutions than small ones. While not quite reaching the sub-micron resolutions of laser-SLA, DLP retains the advantages of lower cost and higher printing speeds [40, 43].

2.3.1. Continuous liquid interface production (CLIP)

Continuous liquid interface production (CLIP) is a type of constrained surface DLP process, where a thin film between building platform and the material tray is not cured and remains liquid. The so-called dead zone at the interface can be generated by utilizing a vat with a floor that is permeable to oxygen. This inhibits curing, and the resin in contact with oxygen remains liquid. Recoating mechanisms are thereby superfluous and continuous elevation of the building platform can be achieved, which improves surface quality and drastically increases printing speed up to 500 mm/h [44]. Similarly, to attain a liquid interface film, a high-density inert and an immiscible liquid layer such as brine has been proposed [45]. CLIP has been commercialized by Carbon Inc., and is establishing itself in the AM market due to its reduced printing times [46].

2.4. Liquid crystal display stereolithography

Since its development in 1997 by Bertsch *et al.* [47], using an LCD device as a dynamic mask for SLA has been almost completely replaced by the DLP counterpart. The latter benefits are from superior switching speeds at higher accuracy [48]. Nevertheless, it merits mentioning as a low-cost alternative to DLP with commercially available LCD printers primarily catering to the laypersons demographic as opposed to the industry [49].

3. Resins in SLA

Photocurable resins for SLA all have the same essential components, as summarized in **Figure 5**. The liquid precursors, which form the network when polymerized, as well as PIs, which start the reaction, are indispensable. In addition, most resin formulations have inert dyes, which absorb incident light and enhance control over the polymerization. Especially when using filled resins, further additives such as diluents, surfactants, or other stabilizers can be present.

3.1. Precursors

The precursors in SLA are liquid molecules, which can be linked together (i.e. polymerized), after exposure to light to form a solid 3D network. Depending on the future application and desired attributes, a variety of monomers, oligomers, or prepolymers can be utilized.
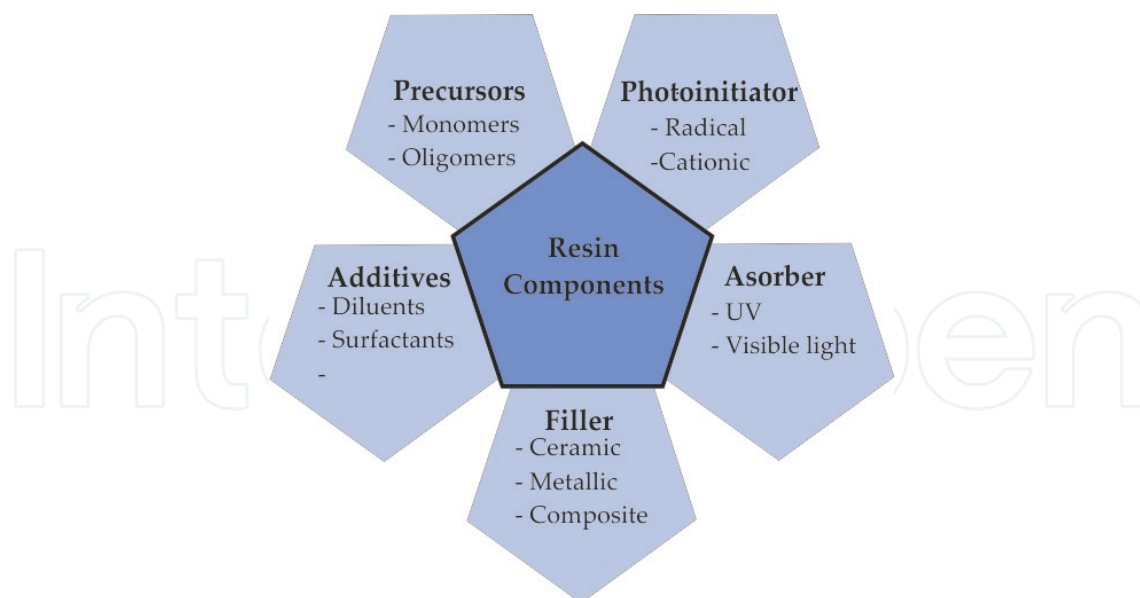
Figure 5. Resin components in SLA.

Acrylate-based resins are common in the SLA process, as they exhibit high reactivities, which is advantageous for fast building speeds [7]. Different types of acrylates are readily available to tune mechanical properties and thermal resistance for example by altering the number of reactive groups [8] or by employing different oligomers such as urethane acrylates [50]. One disadvantage of acrylate resins is their high-shrinkage during printing, causing potential distortion of the printed part. As a solution, the combination with methacrylates is often implemented [51]. The resin's sensitivity to oxygen, which inhibits the polymerization reaction, is another challenge.

Epoxy systems have a different curing mechanism than acrylates. They are based on cationic rather than radical photopolymerization and need longer reaction times, are inhibited by moisture, but have the advantage of stability against oxygen [52]. Additionally, epoxy resins exhibit significantly lower shrinkage than their acrylate counterparts [53]. In order to exploit the advantages of both alternatives, hybrid systems have been created. Combination of acrylate and epoxy-based resins lead to fast curing, low-shrinkage materials and are nowadays the standard in most commercial systems [54, 55].

3.2. Photoinitiators (PIs)

The PI is the resin component, which reacts to light. Once irradiated at the correct wavelength, it is excited and can initiate the curing reaction. A suitable PI, depending on the nature of utilized precursor needs to be selected. Type and amount of PI can substantially influence reaction kinetics, necessary light dosage, conversion, cross-linking density, and by extent, mechanical properties of the printed parts [8, 56, 57].

3.3. Absorbers

Another component that is essential in most SLA processes is a light absorber, which reduces the penetration of light into the resin and limits the depth until, which the resin is cured.

Especially for complex geometries with undercuts, this cure depth needs to be precisely defined in order to prevent excessive curing in z-direction and loss in feature development [14, 17, 40]. The most commonly used UV absorbers are benzotriazole derivatives [58].

3.4. Filled resins

Fabrication of metal or ceramic materials via SLA has been implemented by filling resins with powder, printing the parts, and subsequently debinding and sintering the printed specimens [4, 5], as shown in **Figure 6**. During debinding, the organic resin components are removed by pyrolysis. This binder burnout is easier for thin structures with high filler content, as otherwise, defects such as cracks can form [5]. In the subsequent sintering step, the metal or ceramic powder, which remains, is further thermally treated to achieve dense structures [21]. In order to attain geometrically accurate parts, the material specific shrinkage coefficients need to be taken into account, and high filler content is beneficial to reduce shrinkage [60]. Variations of the thermal treatment include implementing an additional drying step prior to debinding to remove solvents or combining debinding and sintering into one single but correspondingly longer thermal process to eliminate potential defect sources during transportation of the fragile brown parts [59].

Particles smaller than the layer height need to be utilized, and as previously mentioned, maximum particle content is desirable. In highly filled resins with particles in size range of the wavelength of light, scattering is the main interaction mechanism with light and consequently determines cure depth and affects resolution. Reducing the refractive index difference between filler and matrix is a common approach to minimizing scattering [61]. It is noteworthy that composite materials, where the organic component is not removed but retains its matrix function in the final part, have also been manufactured with SLA [3, 62]. By adding (nano)-particles to the SLA resin, mechanical, thermal, optical, or even electrical properties can be further amended [63–65].
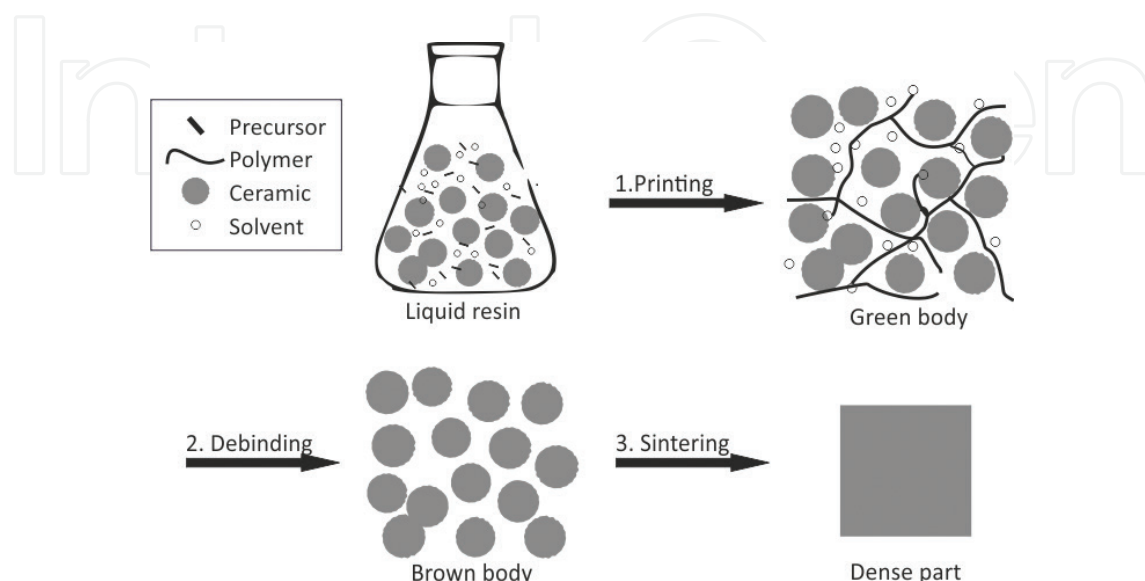

Figure 6. Scheme of the formation of dense ceramic components from filled resins by SLA, redrawn and adapted from [59].

3.5. Additives

A high-volume fraction of solid loading can cause certain disadvantages. Especially for smaller particles with the large surface area, the viscosity of the slurry rises with particle content [4]. This changes the flow behavior of the resin, interferes with coating mechanisms, and increases the mechanical force necessary for the elevation of the building platform in constrained surface setups [19]. Approaches to reduce viscosity include the application of temperature [66], the use of diluents [67], or evoking shear thinning behavior [68].

Rheological additives and stabilizers can increase solid loading and are necessary for extended shelf-life of slurries as well as for stability during longer printing jobs [68]. Agglomeration and sedimentation of particles need to be avoided to ensure continuous, homogeneous ceramic or metal powder distribution. To that end, dispersants such as oligomeric surfactants [69], long chained acids like oleic acid [70], or phosphine oxides with aliphatic chains [71] have been used.

3.6. Post-processing

After removal of the built part from the platform, any support structures that had been necessary for the printing process need to be cut from the green part. Cleaning in suitable solvents and drying of the structure is often followed by sanding of support residues. Post-curing in a UV chamber can be implemented to complete conversion of the polymerization reaction and thereby attain improved mechanical properties [72]. In the case of filled resins, debinding and sintering are the final post-processing steps.

4. Applications

SLA is a very versatile method with applications in a variety of industries. The aerospace and automotive industries can, for instance, benefit from rapid manufacturing of high-performance materials. Microfluidics and medicine are furthermore, significant fields where SLA shows great potential and is already being applied successfully.

Fully polymeric materials structured by SLA can range in their properties from highly elastic silicones for applications in soft robotics [45] to high-strength thermally post-cured epoxy resins [73]. Their limited thermo-mechanical stability is, however, an issue for most polymeric materials. Using filled resins to create metal or ceramic structures, is a possibility in SLA, as previously mentioned in Section 3.4. Furthermore, polymer-derived ceramics can be manufactured by using monomers as precursors, which contain the essential components to form ceramics upon pyrolysis. These methods offer superior versatility in geometry than casting or machining processes and can yield components for high-temperature applications such as in propulsion systems or as thermal insulators [74].

Recently, SLA has been extensively investigated in the field of microfluidics, where small fluid volumes need to be precisely manipulated through micro-sized channels for applications such as inkjet print heads or lab-on-a-chip technologies [6]. When compared to material extrusion and jetting, DLP-SLA shows superior resolution, smaller possible feature sizes,

reduced surface roughness, and faster production times in this application [75]. Channels with dimensions below 100 μm and valves, pumps, as well as multiplexers for mixing [76], can be fabricated rapidly and easily.

Applications in medicine, where patient-specific designs are often necessary to accommodate for individual anatomies, can greatly benefit from AM as well. Some examples are depicted in **Figure 7**. CT or MRI scans can be employed to determine the geometrical specifications, from which devices are then manufactured. Craniofacial implants out of porously structured hydroxyapatite have for example been implanted in patients with large bone defects [80].

In dentistry, CAD modeling has been applied since the 70s in the creation of crowns, which are used to cover a damaged tooth, and dentures, which are removable or fixed devices to replace lost teeth [81]. Now, many AM technologies including SLA can be employed to speed up the process between the acquisition of the geometrical data and implantation of the device into the patient [82]. A second application in healthcare, where AM has become the norm is the manufacturing of hearing aids. SLA can reduce the manufacturing time of these custom-made devices from more than a week to less than a day while also improving wear comfort [83, 84].

Medical applications of SLA are not limited to the fabrication of implants, prostheses, or other medical devices, but drug delivery systems such as micro-needles, capable of administering drugs by painlessly penetrating the skin [78], or 3D printed tablets for individual dosage
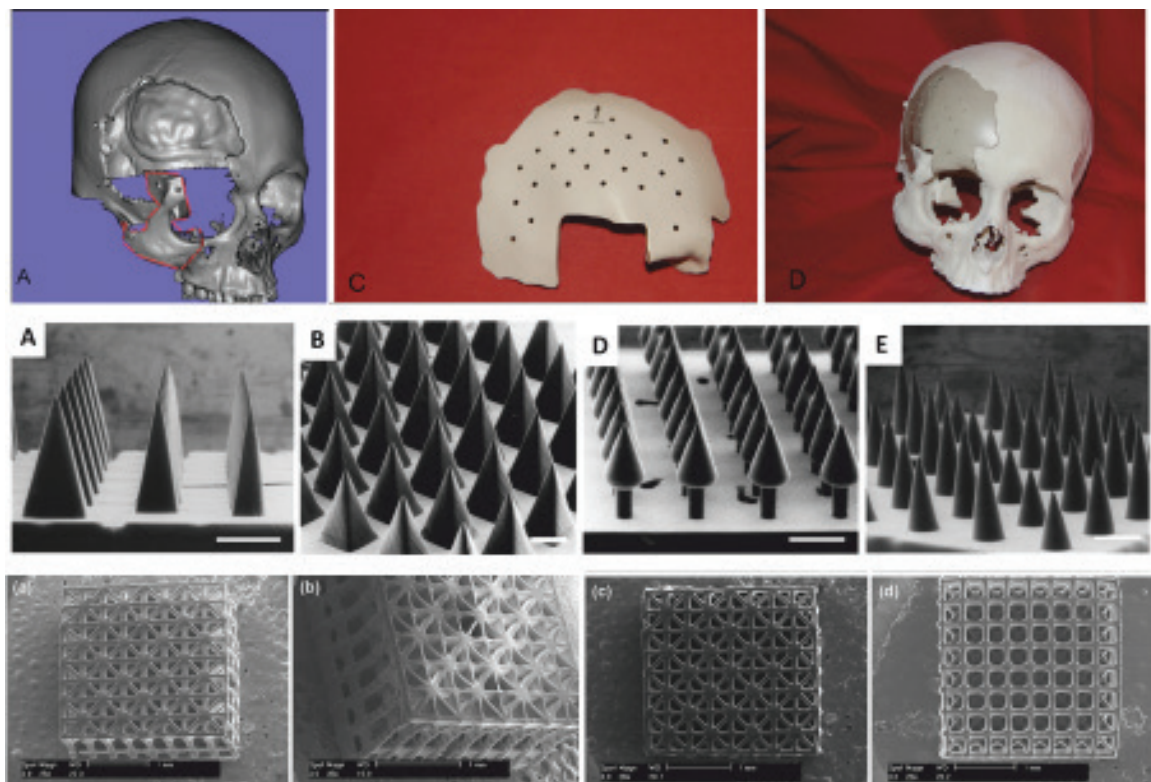

Figure 7. Top row: CAD model of skull defect (A), SLA fabricated cranial implant (C), and an implant placed into skull model (D), reprinted and modified from [77]. Middle row: SEM images of SLA printed microneedle structures for transdermal drug delivery, modified and reprinted from [78]. Bottom row: SEM images of tissue engineering scaffolds for bone regeneration by SLA, modified and reprinted from [79] by permission of Springer Nature.

regulation [85] have also been established. SLA can furthermore be used in medical imaging to create 3D models [86] for preoperative planning [87] or educational purposes [88]. 3D cell culture for more accurate in vitro models to study diseased, as well as healthy tissues, can likewise be created [89]. Tissue engineering constructs in regenerative medicine have also been fabricated with SLA methods [90] and even bioprinting, where live cells are incorporated into the printed scaffold is currently being investigated [91].

5. Commercially available SLA systems

A plethora of SLA printers are currently on the market, ranging in price and quality from amateur desktop applications to professional high-precision machines. A brief overview of their specifications is given in **Table 2**.

LCD-SLA is only available as a low-budget 3D printer for hobbyists. The more common methods such as conventional laser-SLA and DLP-SLA, however, have their low-cost and low-resolution desktop editions for consumers but can also offer high-end methods for professionals and industrial applications. While CLIP and TPP are both in higher price ranges, the former is designed for the extremely fast production of larger parts, while the latter is used for very slow fabrication of small parts with sub-micron resolution.

SLA-type	Lateral resolution (μm)	Printing speed (mm/h)	Maximum print size (mm)	Commercial vendors	Sources
Laser	6–140	14	27–750	3DSystems, Formlabs, XYZPrinting,	[92–95]
TPP	0.400	—	100 × 100 × 3	Nanoscribe	[34]
DLP	33–120	25–150	45–230	EnvisionTEC, Kudo3D	[96–98]
CLIP	50–100	500	80–320	Carbon	[44]
LCD	50–100	20–60	55–160	SparkMaker, Photocentric	[49, 99]

Table 2. Comparison of commercially available SLA systems.

6. Outlook

As the front-runner for high-resolution 3D printing, SLA retains substantial limitations due to the often high costs of this AM method, which are augmented further by slow printing velocities. Additionally, the fact that printing is only possible with one resin at a time severely restricts potential applications.

Trends toward faster manufacturing have already been set by the CLIP technology [44]. Other continuous DLP methods, where building platforms are raised at a constant rate

during the printing process, have also been established [76]. For laser-SLA processes, illumination itself is a limiting factor in reducing printing times and different approaches to increase throughput are necessary. Using a broader scanning pattern for bulk features and applying more precise, narrow lines only in areas where the maximum resolution is required, such as for fine structures and at surfaces, is one method, which is already being implemented [93]. The development of hybrid systems of DLP and laser techniques is currently being investigated as well. Similarly, the inner area should be illuminated via pixel-based DLP, and only round surfaces drawn with the vector-based system of laser-SLA. This could further reduce printing times to rates comparable to DLP while maintaining high-accuracy of laser illumination [22].

Another method, which combines laser and DLP-SLA, addresses the compromise between build size and resolution in DLP. A proposition to retain small pixels and thereby high-resolution even when printing large parts is to laterally stitch the projected images. If a layer has a cross-section exceeding the attainable size by the DMD, it can be divided into smaller areas, which are then illuminated one after the other [100]. This combination of scanning and projection-based illumination, also called large area projection micro SLA (LAPμLA) [101], can lead to the low-cost fabrication of cm-sized objects with a μm-range resolution [102].

Modification of available SLA systems to manufacture parts from multiple materials has been attempted. This usually includes a time consuming cleaning step between material changes. Thus, minimum feature sizes and resolution are no more comparable to conventional SLA than required printing time [103–105]. Nevertheless, after thorough investigation and development, these methods could help to further extend the application spectrum of SLA in the future.

Conflict of interest

None.

Author details

Christina Schmidleithner and Deepak M. Kalaskar*

*Address all correspondence to: d.kalaskar@ucl.ac.uk

University College London, London, United Kingdom

References

[1] Kodama H. Automatic method for fabricating a three-dimensional plastic model with photo-hardening polymer. The Review of Scientific Instruments. 1981;**52**(11):1770-1773

[2] Hull CW. Apparatus for production of three-dimensional objects by stereolithography. 1984. US4575330B1

[3] Wang X, Jiang M, Zhou Z, Gou J, Hui D. 3D printing of polymer matrix composites: A review and prospective. Composites. Part B, Engineering. 2017;**110**:442-458

[4] Bartolo PJ, Gaspar J. Metal filled resin for stereolithography metal part. CIRP Annals. 2008;**57**(1):235-238

[5] Halloran JW. Ceramic Stereolithography: Additive manufacturing for ceramics by photopolymerization. Annual Review of Materials Research. 2016;**46**(1):19-40

[6] Waheed S, Cabot JM, Macdonald NP, Lewis T, Guijt RM, Paull B, et al. 3D printed microfluidic devices: Enablers and barriers. Lab on a Chip. 2016;**16**(11):1993-2013

[7] Ligon SC, Liska R, Stampfl J, Gurr M, Mülhaupt R. Polymers for 3D printing and customized additive manufacturing. Chemical Reviews. 2017;**117**(15):10212-10290

[8] Stampfl J, Baudis S, Heller C, Liska R, Neumeister A, Kling R, et al. Photopolymers with tunable mechanical properties processed by laser-based high-resolution stereolithography. Journal of Micromechanics and Microengineering. 2008;**18**(12):125014

[9] Lee JM, Zhang M, Yeong WY. Characterization and evaluation of 3D printed microfluidic chip for cell processing. Microfluidics and Nanofluidics. 2016;**20**(1):5

[10] Launhardt M, Wörz AW, Loderer A, Laumer T, Drummer D, Hausotte T, et al. Detecting surface roughness on SLS parts with various measuring techniques. Polym Test. 2016;**53**:217-226

[11] Quake SR, Scherer A. From micro- to nanofabrication with soft materials. Science. 2000 Nov 24;**290**(5496):1536-1540

[12] Xia Y, Whitesides GM. Soft lithography. Angewandte Chemie International Edition. 1998;**37**(5):550-575

[13] ASTM ISO/ASTM52921-13 Standard Terminology for Additive Manufacturing-Coordinate Systems and Test Methodologies. West Conshohocken: ASTM International; 2013

[14] Han L-H, Mapili G, Chen S, Roy K. Projection microfabrication of three-dimensional scaffolds for tissue engineering. Journal of Manufacturing Science and Engineering. 2008;**130**(2):21005

[15] Pan Y, Zhou C, Chen Y. A fast mask projection Stereolithography process for fabricating digital models in minutes. Journal of Manufacturing Science and Engineering. 2012;**134**(5):51011

[16] Huang Y-M, Kuriyama S, Jiang C-P. Fundamental study and theoretical analysis in a constrained-surface stereolithography system. International Journal of Advanced Manufacturing Technology. 2004;**24**(5-6):361-369

[17] Choi J, Wicker RB, Cho S, Ha C, Lee S. Cure depth control for complex 3D microstructure fabrication in dynamic mask projection microstereolithography. Rapid Prototyping Journal. 2009;**15**(1):59-70

[18] Hatzenbichler M, Geppert M, Seemann R, Stampfl J. Additive manufacturing of photopolymers using the Texas Instruments DLP lightcrafter. In: Proceedings of SPIE, Emerging Digital Micromirror Device Based Systems and Applications V. San Francisco: International Society for Optics and Photonics; 2013. pp. 86180A

[19] Huang Y-M, Jiang C-P. On-line force monitoring of platform ascending rapid prototyping system. Journal of Materials Processing Technology. 2005;**159**(2):257-264

[20] Chen Y, Zhou C. Digital mask-image-projection-based additive manufacturing that applies shearing force to detach each added layer. 2013. US13872954

[21] Schwentenwein M, Homa J. Additive manufacturing of dense alumina ceramics. International Journal of Applied Ceramic Technology. 2015;**12**(1):1-7

[22] Busetti B, Lutzer B, Stampfl J. Development of a hybrid exposure system for lithographybased additive manufacturing technologies. In: Laser 3D Manufacturing V. San Francisco: International Society for Optics and Photonics; 2018. p. 4

[23] Xia C, Fang NX. 3D microfabricated bioreactor with capillaries. Biomedical Microdevices. 2009;**11**(6):1309-1315

[24] Lee IH, Cho DW. Micro-stereolithography photopolymer solidification patterns for various laser beam exposure conditions. International Journal of Advanced Manufacturing Technology. 2003;**22**(5-6):410-416

[25] Zhang X, Jiang XN, Sun C. Micro-stereolithography of polymeric and ceramic microstructures. Sensors and Actuators A: Physical. 1999;**77**(2):149-156

[26] Denk W, Strickler JH, Webb WW. Two-photon laser scanning fluorescence microscopy. Science. 1990;**248**(4951):73-76

[27] Takada K, Sun H-B, Kawata S. Improved spatial resolution and surface roughness in photopolymerization-based laser nanowriting. Applied Physics Letters. 2005;**86**(7):71122

[28] Park S-H, Yang D-Y, Lee K-S. Two-photon stereolithography for realizing ultraprecise three-dimensional nano/microdevices. Laser & Photonics Reviews. 2009;**3**(1-2):1-11

[29] Das Unternehmen im Detail – Nanoscribe GmbH [Internet]. [cited 2018 Mar 10]. Available from: https://www.nanoscribe.de/de/unternehmen/

[30] Serbin J, Egbert A, Ostendorf A, Chichkov BN, Houbertz R, Domann G, et al. Femtosecond laser-induced two-photon polymerization of inorganic-organic hybrid materials for applications in photonics. Optics Letters. 2003;**28**(5):301-303

[31] Maruo S, Nakamura O, Kawata S. Three-dimensional microfabrication with two-photon-absorbed photopolymerization. Optics Letters. 1997;**22**(2):132

[32] Ovsianikov A, Viertl J, Chichkov B, Oubaha M, MacCraith B, Sakellari I, et al. Ultra-low shrinkage hybrid photosensitive material for two-photon polymerization microfabrication. ACS Nano. 2008;**2**(11):2257-2262

[33] Wu S, Serbin J, Gu M. Two-photon polymerisation for three-dimensional micro-fabrication. Journal of Photochemistry and Photobiology A: Chemistry. 2006;**181**(1):1-11

[34] Data sheet: Photonic Professional G T [Internet]. [cited 2018 Mar 14]. Available from: https://www.nanoscribe.de/files/2715/1912/9082/DataSheet_Photonic_Professional_GT.pdf

[35] Pucher N, Rosspeintner A, Satzinger V, Schmidt V, Gescheidt G, Stampfl J, et al. Structure–activity relationship in D-π-A-π-D-based photoinitiators for the two-photon-induced photopolymerization process. Macromolecules. 2009;**42**(17):6519-6528

[36] Ikuta K, Maruo S, Kojima S. New micro stereo lithography for freely movable 3D micro structure-super IH process with submicron resolution. In: Proceedings of the IEEE International Conference on Micro Electro Mechanical Systems (MEMS). Heidelberg: IEEE; 1998. p. 290-295

[37] Maruo S, Ikuta K. Submicron stereolithography for the production of freely movable mechanisms by using single-photon polymerization. Sensors and Actuators A: Physical. 2002;**100**(1):70-76

[38] Gandhi P, Bhole K. Characterization of "bulk lithography" process for fabrication of three-dimensional microstructures. Journal of Micro and Nano-Manufacturing. 2013;**1**(4):41002

[39] Gandhi P, Bhole K, Chaudhari N. Fabrication of textured 3D microstructures using "bulk lithography". In: ASME 2012 International Manufacturing Science and Engineering Conference. ASME; 2012. pp. 959

[40] Sun C, Fang N, Wu DM, Zhang X. Projection micro-stereolithography using digital micro-mirror dynamic mask. Sensors and Actuators A: Physical. 2005;**121**(1):113-120

[41] Macdonald NP, Bunton GL, Park AY, Breadmore MC, Kilah NL. 3D printed micrometer-scale polymer mounts for single crystal analysis. Analytical Chemistry. 2017;**89**(8):4405-4408

[42] Katal G, Tyagi N, Joshi A. Digital light processing and its future applications. International Journal of Scientific and Research Publications. 2013;**3**(1):2250-3153

[43] Baumgartner S, Pfaffinger M, Busetti B, Stampfl J. Comparison of Dynamic Mask- And Vector-Based Ceramic Stereolithography. In: Proceedings of the 41st International Conference on Advanced Ceramics and Composites. Hoboken: Wiley; 2018. P. 163-173

[44] Tumbleston JR, Shirvanyants D, Ermoshkin N, Januszwiewiez R, Johnsn AR, Kelly D, et al. Continuous liquid interface production of 3D objects. Science. 2015;**347**(6228):1349-1352

[45] Thrasher CJ, Schwartz JJ, Boydston AJ. Modular elastomer Photoresins for digital light processing additive manufacturing. ACS Applied Materials & Interfaces. 2017;**9**(45):39708-39716

[46] Process – Carbon [Internet]. [cited 2018 Mar 11]. Available from: https://www.carbon3d.com/process/

[47] Bertsch A, Zissi S, Jézéquel JY, Corbel S, André JC. Microstereophotolithography using a liquid crystal display as dynamic mask-generator. Microsystem Technologies. 1997 Feb 21;**3**(2):42-47

[48] Hornbeck LJ. The DMDTM Projection Display Chip: A MEMS-Based Technology. MRS Bull. 2001;**26**(4):325-327

[49] SparkMaker [Internet]. [cited 2018 Mar 11]. Available from: https://www.sparkmaker3d.com/

[50] Coats AL, Harrison JP, Hay JS, Ramos Manuel Jacinto. Stereolithography resins and methods. 2003. US10628304

[51] Murphy EJ, Ansel RE, Krajewski JJ. Method of forming a three-dimensional object by stereolithography and composition therefore. 1989. US07429568

[52] Sipani V, Scranton AB. Kinetic studies of cationic photopolymerizations of phenyl glycidyl ether: Termination/trapping rate constants for iodonium photoinitiators. Journal of Photochemistry and Photobiology A: Chemistry. 2003;**159**(2):189-195

[53] Esposito Corcione C, Greco A, Maffezzoli A. Photopolymerization kinetics of an epoxy-based resin for stereolithography. Journal of Applied Polymer Science. 2004;**92**(6):3484-3491

[54] Lee TY, Carioscia J, Smith Z, Bowman CN. Thiol-Allyl Ether-Methacrylate Ternary Systems. Evolution Mechanism of Polymerization-Induced Shrinkage Stress and Mechanical Properties. Macromolecules. 2007;**40**(5):1473-1479

[55] Zhiwei G, Jianhua M, Shuhuai H, Hongquan X. Development of a hybrid photopolymer for stereolithography. Journal of Wuhan University of Technology-Materials Science Edition. 2006;**21**(1):99-101

[56] Badev A, Abouliatim Y, Chartier T, Lecamp L, Lebaudy P, Chaput C, et al. Photopolymerization kinetics of a polyether acrylate in the presence of ceramic fillers used in stereolithography. Journal of Photochemistry and Photobiology A: Chemistry. 2011;**222**(1):117-122

[57] Bail R, Patel A, Yang H, Rogers CM, Rose FRAJ, Segal JI, et al. The effect of a type I photoinitiator on cure kinetics and cell toxicity in projection-microstereolithography. Procedia CIRP. 2013;**5**:222-225

[58] Bail R, Hong JY, Chin BD. Effect of a red-shifted benzotriazole UV absorber on curing depth and kinetics in visible light initiated photopolymer resins for 3D printing. Journal of Industrial and Engineering Chemistry. 2016;**38**:141-145

[59] de Blas Romero A, Pfaffinger M, Mitteramskogler G, Schwentenwein M, Jellinek C, Homa J, et al. Lithography-based additive manufacture of ceramic biodevices with design-controlled surface topographies. International Journal of Advanced Manufacturing Technology. 2017;**88**(5-8):1547-1555

[60] Hinczewski C, Corbel S, Chartier T. Ceramic suspensions suitable for stereolithography. Journal of the European Ceramic Society. 1998;**18**(6):583-590

[61] Griffith ML, Halloran JW. Scattering of ultraviolet radiation in turbid suspensions Prediction of ceramic stereolithography resin sensitivity from theory and measurement of diffusive photon Scattering of ultraviolet radiation in turbid suspensions. Journal of Applied Physics. 1997;**81**(47):2538-24902

[62] Manjubala I, Woesz A, Pilz C, Rumpler M, Fratzl-Zelman N, Roschger P, et al. Biomimetic mineral-organic composite scaffolds with controlled internal architecture. Journal of Materials Science: Materials in Medicine. 2005;**16**(12):1111-1119

[63] Farahani RD, Dubé M, Therriault D. Three-dimensional printing of multifunctional nanocomposites: Manufacturing techniques and applications. Advanced Materials. 2016;**28**(28):5794-5821

[64] Lin D, Jin S, Zhang F, Wang C, Wang Y, Zhou C, et al. 3D stereolithography printing of graphene oxide reinforced complex architectures. Nanotechnology. 2015;**26**(43):434003

[65] Credi C, Fiorese A, Tironi M, Bernasconi R, Magagnin L, Levi M, et al. 3D printing of cantilever-type microstructures by stereolithography of ferromagnetic photopolymers. ACS Applied Materials & Interfaces. 2016;**8**(39):26332-26342

[66] Tomeckova V, Halloran JW. Flow behavior of polymerizable ceramic suspensions as function of ceramic volume fraction and temperature. Journal of the European Ceramic Society. 2011;**31**(14):2535-2542

[67] Melchels FPW, Feijen J, Grijpma DW. A review on stereolithography and its applications in biomedical engineering. Biomaterials. 2010;**31**(24):6121-6130

[68] De Hazan Y, Heinecke J, Weber A, Graule T. High solids loading ceramic colloidal dispersions in UV curable media via comb-polyelectrolyte surfactants. Journal of Colloid and Interface Science. 2009;**337**(1):66-74

[69] Teng WD, Edirisinghe MJ, Evans JRG. Optimization of dispersion and viscosity of a ceramic jet printing ink. Journal of the American Ceramic Society. 1997;**80**(2):486-494

[70] Li K, Zhao Z. The effect of the surfactants on the formulation of UV-curable SLA alumina suspension. Ceramics International. 2017;**43**(6):4761-4767

[71] Goswami A, Ankit K, Balashanmugam N, Umarji AM, Madras G. Optimization of rheological properties of photopolymerizable alumina suspensions for ceramic microstereolithography. Ceramics International. 2014;**40**(2):3655-3665

[72] Kim H-C, Lee S-H. Reduction of post-processing for stereolithography systems by fabrication-direction optimization. Computer Design. 2005;**37**(7):711-725

[73] Kuang X, Zhao Z, Chen K, Fang D, Kang G, Qi HJ. High-Speed 3D Printing of High-Performance Thermosetting Polymers via Two-Stage Curing. Macromol Rapid Commun. 2018;**39**(7):1700809

[74] Eckel ZC, Zhou C, Martin JH, Jacobsen AJ, Carter WB, Schaedler TA. Additive manufacturing of polymer-derived ceramics. Science. 2016;**351**(6268):58-62

[75] Macdonald NP, Cabot JM, Smejkal P, Guijt RM, Paull B, Breadmore MC. Comparing microfluidic performance of three-dimensional (3D) printing platforms. Analytical Chemistry. 2017;**89**(7):3858-3866

[76] Gong H, Woolley AT, Nordin GP. High density 3D printed microfluidic valves, pumps, and multiplexers. Lab on a Chip. 2016;**16**(13):2450-2458

[77] Kumta S, Kumta M, Jain L, Purohit S, Ummul R. A novel 3D template for mandible and maxilla reconstruction: Rapid prototyping using stereolithography. Indian Journal of Plastic Surgery. 2015;**48**(3):263-273

[78] Johnson AR, Caudill CL, Tumbleston JR, Bloomquist CJ, Moga KA, Ermoshkin A, et al. Single-step fabrication of computationally designed microneedles by continuous liquid Interface production. Yamamoto M, editor. PLoS One. 2016;**11**(9):1-17

[79] Lan PX, Lee JW, Seol Y-J, Cho D-W. Development of 3D PPF/DEF scaffolds using micro-stereolithography and surface modification. Journal of Materials Science. Materials in Medicine. 2009;**20**(1):271-279

[80] Brie J, Chartier T, Chaput C, Delage C, Pradeau B, Caire F, et al. A new custom made bioceramic implant for the repair of large and complex craniofacial bone defects. Journal of Cranio-Maxillo-Facial Surgery. 2013;**41**(5):403-407

[81] Miyazaki T, Hotta Y, Kunii J, Kuriyama S, Tamaki Y. A review of dental CAD/CAM: Current status and future perspectives from 20 years of experience. Dental Materials Journal. 2009;**28**(1):44-56

[82] Bhargav A, Sanjairaj V, Rosa V, Wen Feng L, Fuh JY. Applications of additive manufacturing in dentistry: A review. Journal of Biomedical Materials Research Part B: Applied Biomaterials. 2017

[83] Dodziuk H. Applications of 3D printing in healthcare. Kardiochirurgia i Torakochirurgia Polska/Polish Journal of Thoracic and Cardiovascular Surgery. 2016;**13**(3):283-293

[84] Chrzan R, Miechowicz S, Urbanik A, Markowska O, Kudasik T. Individually fitted hearing aid device manufactured using rapid prototyping based on ear CT a case report. The Neuroradiology Journal. 2009;**22**:209-214

[85] Alhnan MA, Okwuosa TC, Sadia M, Wan K-W, Ahmed W, Arafat B. Emergence of 3D printed dosage forms: Opportunities and challenges. Pharmaceutical Research. 2016;**33**(8):1817-1832

[86] Marro A, Bandukwala T, Mak W. Three-dimensional printing and medical imaging: A review of the methods and applications. Current Problems in Diagnostic Radiology. 2016;**45**(1):2-9

[87] Chae MP, Rozen WM, McMenamin PG, Findlay MW, Spychal RT, Hunter-Smith DJ. Emerging applications of bedside 3D printing in plastic surgery. Frontiers in Surgery. 2015;**2**:25

[88] Dhir V, Itoi T, Fockens P, Perez-Miranda M, Khashab MA, Seo DW, et al. Novel ex vivo model for hands-on teaching of and training in EUS-guided biliary drainage: Creation of "Mumbai EUS" stereolithography/3D printing bile duct prototype (with videos). Gastrointestinal Endoscopy. 2015;**81**(2):440-446

[89] Neiman JAS, Raman R, Chan V, Rhoads MG, Raredon MSB, Velazquez JJ, et al. Photopatterning of hydrogel scaffolds coupled to filter materials using stereolithography for perfused 3D culture of hepatocytes. Biotechnology and Bioengineering. 2015;**2**(4):777-787

[90] Mota C, Puppi D, Chiellini F, Chiellini E. Additive manufacturing techniques for the production of tissue engineering constructs. Journal of Tissue Engineering and Regenerative Medicine. 2015;**9**(3):174-190

[91] Shanjani Y, Pan CC, Elomaa L, Yang Y. A novel bioprinting method and system for forming hybrid tissue engineering constructs. Biofabrication. 2015 Dec 18;**7**(4):45008

[92] ProJet® 1200 Micro-SLA Printer [Internet]. [cited 2018 Mar 14]. Available from: http://www.cadventure.co.uk/wp-content/uploads/2017/06/3D-Systems_Micro-SLA_ProJet_1200_Tech_Specs_USEN_2016.12.01_a_WEB.pdf

[93] 3D Stereolithography Printers [Internet]. [cited 2018 Mar 14]. Available from: https://www.3dsystems.com/sites/default/files/2017-05/3D-Systems_SLA_Specsheet_A4_US_2017.05.16_WEB.pdf

[94] Technische Daten | Formlabs [Internet]. [cited 2018 Mar 14]. Available from: https://formlabs.com/de/3d-printers/technische-daten/

[95] Nobel 1.0A | SL 3D Printer | 3D Printer |XYZprinting [Internet]. [cited 2018 Mar 14]. Available from: https://www.xyzprinting.com/en-US/product/nobel-1-0a

[96] Micro Plus cDLM [Internet]. [cited 2018 Mar 14]. Available from: https://envisiontec.com/wp-content/uploads/2016/09/2017-Micro-Plus-cDLM.pdf

[97] 3D printer – Wanhao [Internet]. [cited 2018 Mar 14]. Available from: http://www.wanhao3dprinter.com/

[98] High Resolution 3D Printer – SLA DLP – Kudo3D Inc. [Internet]. [cited 2018 Mar 14]. Available from: https://www.kudo3d.com/

[99] Liquid Crystal Precision – Photocentric Group [Internet]. [cited 2018 Mar 14]. Available from: https://photocentricgroup.com/lcprecision/?v=fa868488740a

[100] Lee MP, Cooper GJT, Hinkley T, Gibson GM, Padgett MJ, Cronin L. Development of a 3D printer using scanning projection stereolithography. Scientific Reports. 2015 Sep 23;**5**(1):9875

[101] Moran BD. Large area projection micro stereolithography. 2015. US14688187

[102] Zheng X, Smith W, Jackson J, Moran B, Cui H, Chen D, et al. Multiscale metallic metamaterials. Nature Materials. 2016 Oct 18;**15**(10):1100-1106

[103] Zhou C, Chen Y, Yang Z, Khoshnevis B, Epstein DJ. Digital material fabrication using mask-image-projection- based stereolithography. Rapid Prototyping Journal. 2013;**19**(3):153-165

[104] Choi J-W, Kim H-C, Wicker R. Multi-material stereolithography. Journal of Materials Processing Technology. 2011 Mar 1;**211**(3):318-328

[105] Arcaute K, Mann B, Wicker R. Stereolithography of spatially controlled multi-material bioactive poly(ethylene glycol) scaffolds. Acta Biomaterialia. 2010 Mar 1;**6**(3):1047-1054